Available online at www.sciencedirect.com

jmr&t Journal of Materials Research and Technology

www.jmrt.com.br

Review Article

Equivalent material model of corroded prestressing steel strand

*Chi-Ho Jeon, Jae-Bin Lee, Sokanya Lon, Chang-Su Shim**

Department of Civil and Environmental Engineering, Chung-Ang University, Seoul, Republic of Korea

ARTICLE INFO

Article history:
20 April 2019

Keywords:
Prestressed concrete bridge
Prestressing steel
Corrosion
Section loss
Strength
Ductility

ABSTRACT

One of the main load resisting elements in prestressed concrete bridges is prestressing steel. Corrosion of the prestressing steel is generally protected by grouting and duct. Even though the strand is crucial, it is difficult to visually inspect the corrosion. In this paper, corrosion of the strand is classified into three types according to observation of corroded strands from existing bridges. Equations for section loss of the corroded strand were suggested. Mechanical properties of the corroded strand such as strength and ductility were estimated by tensile test. Finite element analysis on the corroded wire and the proposed spring model provided equivalent stress–strain models for corroded prestressing steel. The suggested models were verified by the tensile tests and can be utilised for the analysis of prestressed concrete members with corroded strands.

© 2019 The Authors. Published by Elsevier B.V. This is an open access article under the CC BY-NC-ND license (http://creativecommons.org/licenses/by-nc-nd/4.0/).



Changsu Shim is a professor on structural engineering at Chung-Ang University, Korea. He received his Ph.D on pre-cast deck structures from Seoul National University, Korea. His research includes connections of modular structures, digital modelling technologies and assessment of existing structures. Currently, he is the president of Korean BIM institute.

1. Introduction

The loss of load carrying capacity, stiffness, and ductility in concrete structure due to corrosion has been studied by many researchers. The corrosion of steel is basically caused by chemical reaction between iron ions, water, and oxygen. The reinforcements inside the concrete in normal condition are protected by the passive film from the corrosion chemical reaction, which is generally formed above the PH level of 11.5 [1]. However, if the PH level drops from the surround environmental condition changed due to crack, carbonation, and so on, the reinforcement is exposed to air and begins to be corroded. This is called depassivation, and the larger area where this phenomenon appears, the greater the corrosion reaction occurs [2].

According to review study on the corrosion of reinforcement [3], the corrosion of steel in concrete can be classified into two major categories which are external factors and

* *Corresponding author.*
E-mails: chihobeer@cau.ac.kr (C. Jeon), jbest90@cau.ac.kr (J. Lee), lonsokanya1993@cau.ac.kr (S. Lon), csshim@cau.ac.kr (C. Shim).
https://doi.org/10.1016/j.jmrt.2019.02.010
2238-7854/© 2019 The Authors. Published by Elsevier B.V. This is an open access article under the CC BY-NC-ND license (http://creativecommons.org/licenses/by-nc-nd/4.0/).

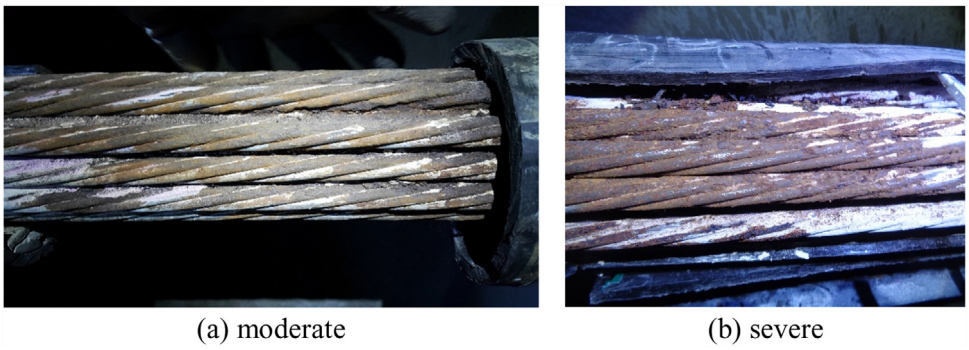

Fig. 1 – Prestressing steel corrosion in external tendon.

internal factors. The internal factors are mostly environmental factors at the level of the steel inside the concrete; oxygen, relative humidity, temperature, carbonation, acidic gaseous pollutants, and chloride ions. These factors can reduce the PH level and lead to chemical reaction of corrosion. The external factors are related to the quality parameters of concrete and steel; cement content, admixtures, curing water, aggregates including chloride salts, w/c ratio, chemical composition and structure of reinforcing steel.

The technical report from FHWA [4] introduced the cases of prestressing steel strand fracture at existing bridges, and it is found that the corrosion of prestressing steel in duct mostly occurs at two weak locations; void in duct and anchorage. First, the void in the duct is formed when the grout is not sufficiently filled or makes bleeding water, which causes the strands is exposed to air. The cases of corrosion due to void were found at Mid-Bay Bridge and Ringling Bridge. Another reason of the stand corrosion is insufficient sealing of anchorage. The anchorage zone is the most exposed part to external environment especially when it is located at an expansion joint. Therefore, it can be the path of infiltration of chloride-contaminated water if the anchorage contains voids. This corrosion phenomenon was found at Sunshine Skyway Bridge and Niles Channel Bridge. Fig. 1 shows the typical corrosion of the external tendons after uncovering the duct.

As the strand corrosion has emerged as an issue, many researches have been conducted to evaluate the performance of the corrosion strand. Existing classification of corroded strands introduced in U.S were made by visual inspection [4–6]. This method was used to visual inspection of Varina-Enon Bridge. The quantitative evaluation method for corrosion damage was introduced in ASTM standard [7]. This method is based on mass loss and exposed time, therefore, this suggestion is hard to be adopted in this paper, because measuring mass is impossible method in the practical inspection. WU and LI [8] suggested mechanical performance of corroded prestressing steel strand. The corrosion on the strand specimens occurred artificially using salt spray test, and the mechanical performance is with respect to the extent of corrosion measured by mass loss. Lu et al. [9] suggested prediction models of the mechanical behaviour of corroded strands. The measuring method of extent of corrosion was based on reduced geometric sectional area with pitting depth.

In this paper, advanced prediction model of the mechanical behaviour of corroded strands is suggested. The extent of corrosion of a wire is based on the loss of sectional area with pitting depth with respect to three types of pit configuration. The mechanical behaviour of the wires were analysed by finite element method, and the behaviour of seven-wire strand was predicted using equivalent spring model. The prediction models were compared to the results of tensile tests.

2. Corrosion inspection and section loss

2.1. *Corrosion inspection*

In this paper, prestressing steel strands in external tendons of existing bridge were inspected for the corrosion. The inspected bridge has 12 external tendons, and each tendon has 19 strands. Because the steel strand is surrounded by grout and duct, it is hard to know whether it is corroded. The sounding inspection, therefore, was conducted with hitting rod to find out the location of void in ducts. Once a large void had been detected from sounding inspection, duct was opened for the detailed visual inspection. The occurrence of voids was mainly found in the upper bent part of the tendon profile because the air and bleeding water in the grout collects at the top. The corrosion occurred mainly at the upper bent part where has void as large as strands exposed to air, which was similar to the corrosion cases introduced in FHWA report [4]. The extent of corrosion was related to the amount of reaming grout. Entirely protected part of the strands had no corrosion at all even though other strands were severely corroded in a cross section of a tendon.

The visual inspection of corroded strands [4–6] was attempted, however, it was hard to judge whether the corroded strands must be replaced, because extent of corrosion was varied according to investigators. This led to the need for quantitative method, and predicting mechanical performance using pitting depth has attempted thereby. Among the measuring method of pitting depth in ASTM G46-94 [10], using pit depth gauge was selected (see Fig. 2). This method is relatively easier and faster to apply to field inspection than others as microscopic and metallographic methods. The needle inside the pit depth gauge comes out from middle of the base plate reaches the corroded surface of a wire, and the distance from



Fig. 2 – Measuring pit depth of corroded wire.

base plate to needle tip is measured. The deepest location of the pit was, of course, hard be found. Therefore, several times of measurement had been conducted at the same location until the deepest depth was specified. The corroded surface of strands had been cleaned before it is measured. After 7 wires in a section that had the largest loss area were measured, quantitative sectional loss of the strand has been evaluated by the method introducing in this paper.

2.2. *Evaluation of section loss according to pit configuration*

The extent of corrosion is the most important parameter to evaluate the mechanical behaviour of corroded strand. In the electrochemistry, that is generally defined by mass loss [8,11,12]. This method, however, may not be accurate when the corrosion spread widely, because the behaviour of strand is governed by the most corroded section with smallest area. On the other hand, section loss can be more directive factor to evaluate the mechanical behaviour. Several researchers suggested corrosion shape called pit configurations in order to facilitate the calculation of the cross-sectional loss. Lu et al. suggested hemispherical pit configuration [9] based on Val and Melchers model [13]. Stewart also proposed similar shape of pit configuration in rebar [14]. Hartt and Lee proposed planar pit configuration [15]. These assumptions have the advantage that the cross-sectional loss can be defined in relation to the pit depth but disadvantage that single configuration can explain only the similar pit configuration. The definition of pit configuration in this paper is intended to figure out the section loss so that inspector can make relatively accurate judgement on the severity of the corroded strands, and the inspector can visually recognise the corrosion shapes without additional inspection.

In order to explain the behaviour of corroded strand, corrosion shapes have been analysed from observation of the real corroded strands in this paper, and that resulted in three representative models of pit configuration as shown in Fig. 3. The section photos depict real corrosion shape of corroded wire corresponding to the types. The grey area in the figure is the residual cross-sectional area.

The loss of sectional area can be calculated through Eqs. (1)–(6).

$$A_{sl,1} = 2r^2\left(\theta_1 - \sin\theta_1\cos\theta_1\right) \quad for \quad 0 \le d_p \le 2r \tag{1}$$

$$\theta_1 = \arccos\left(1 - \frac{d_p}{2r}\right) \tag{2}$$

$$A_{sl,2} = r^2\left(2\theta_2 - \pi - 2\sin\theta_2\cos\theta_2\right) \quad for \quad 0 \le d_p \le 2r \tag{3}$$

$$\theta_2 = \arccos\left(-\frac{d_p}{2r}\right) \tag{4}$$

$$A_{sl,3} = r^2\left(\theta_3 - \sin\theta_3\cos\theta_3\right) \quad for \quad 0 \le d_p \le 2r \tag{5}$$

$$\theta_3 = \arccos\left(1 - \frac{d_p}{r}\right) \tag{6}$$

$A_{sl,1-3}$ are the loss of sectional area according to the type of pit configuration, r is the radius of a wire, and d_p is the pit depth measured by depth gauge at the deepest location.

3. Tensile test of corroded strand

3.1. *Test specimens*

A total of 16 seven wire strands (3 non-corroded strands and 13 corroded strands) were collected with length of 800–1000 mm from existing bridge. The strand has nominal diameter of 15.2 mm and sectional-area of 138.7 mm. The radius of a wire is 2.6 mm for the core wire and 2.5 mm for outer wires. From the tensile test of non-corroded strands, the tensile strength and elongation were found as 1865 MPa and 75,000 $\mu\varepsilon$, respectively. Before tests were conducted, they were cleaned with steel brush and rust remover. Inspection to evaluate the section loss was also conducted along the length of the specimen with pit depth gauge so that the location of the most corroded section be found. For the quantitative comparison of corrosion, the extent of section loss, denoted as η, was expressed as follows:

$$\eta = \frac{A_{sl}}{A_0} \tag{7}$$

where A_0 is the sectional area of a wire, and A_{sl} is the loss of sectional area from Eqs. (1)–(6).

Each wire has own pit depth and pit configuration, therefore, section loss should be evaluated six times to calculate the section loss of a strand (A strand has six outer wires and one core wire. The core wire is hard to be measured and mostly not corroded). Total section loss of a strand is the sum of section loss of six wires. Table 1 shows the list of test specimens with section loss of the most corroded wire among the seven wires in a cross section and section loss the strands at the cross section. In the previous research on the corroded strands, the strength capacity was reduced up to 7.4% even in moderate corrosion [16], and the Specification for Grouting of Post-Tensioned Structures from PTI [17] suggested prestressing steel be rejected if pit is larger than 0.002 in. Therefore, the target of corrosion degree in this paper is set strictly, and this

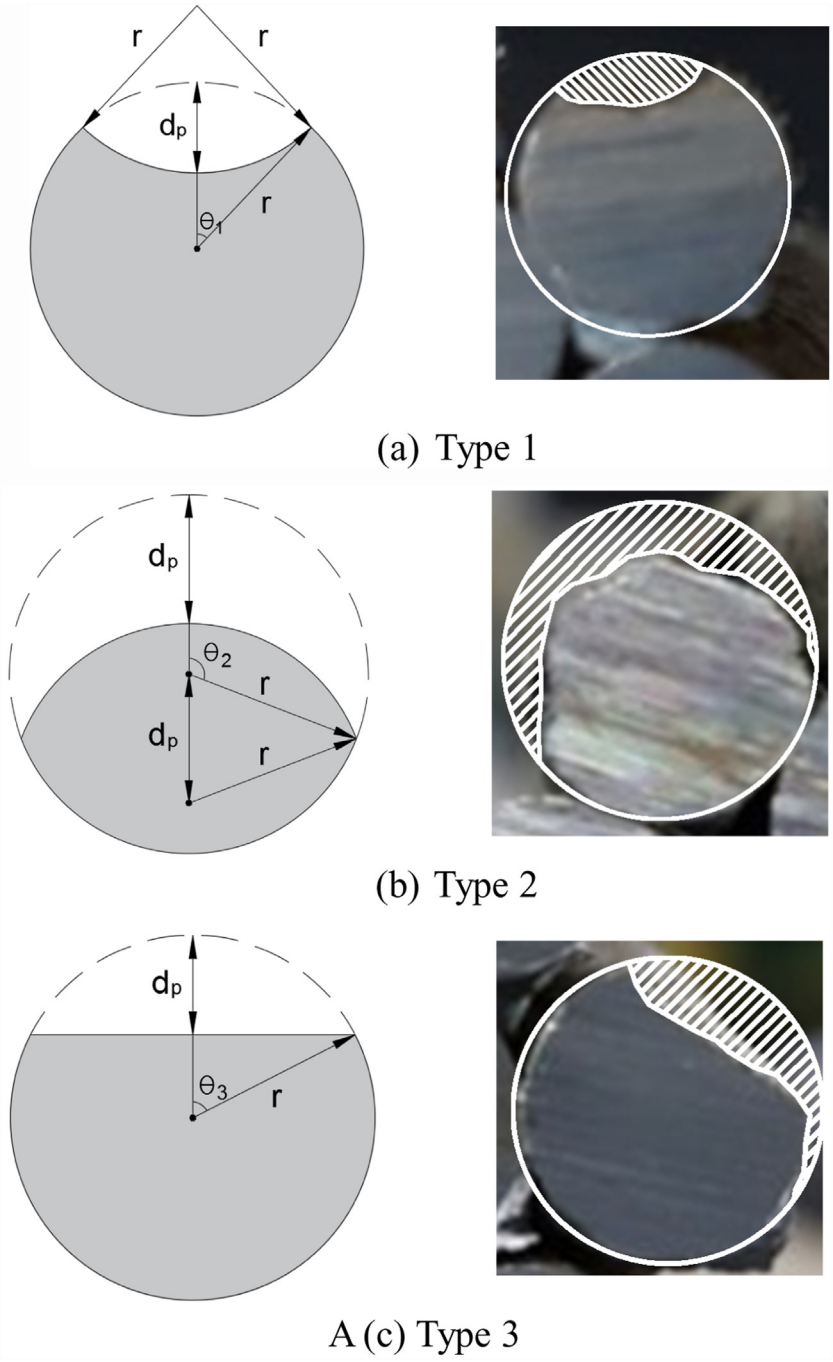

Fig. 3 – Pit configurations.

paper also shows the corrosion level of wire is more important than the section of a strand.

3.2. *Tensile test*

The tensile tests were conducted with a universal testing machine as shown in Fig. 4(a). The specimens were loaded up to their failure by displacement control method with speed of 5 mm/min. The failure of corrosion was defined as a moment that even a wire is broke. In the tensile test, two end sides of the strand are held by the grip. If the grip wedge contacts the surface of a strand directly, crack can be propagated from the wedge earlier than the tensile strength of the wire due to stress concentration. For this reason, Kim et al. [18] suggested to wrap the end parts with silica-coated aluminium foil to protect the end parts. This method was adopted in this paper.

The elongation was measured by extracted data from the machine, not extensometer because sudden rupture of a strand can make damage. To verify the reliability of the data, 11 corroded specimens were tested preliminarily with 100 mm distance of marker (see Fig. 4(b)) at the most likely failure

Table 1 – List of test specimens.

Specimen	Section loss (%)	
	Most corroded wire (TPC)	Strand
NCS 1	–	–
NCS 2	–	–
NCS 3	–	–
CS 1	2.21 (3)	0.30
CS 2	1.05 (3)	0.13
CS 3	20.28 (2)	3.83
CS 4	17.91 (1)	3.23
CS 5	12.24 (3)	2.90
CS 6	6.42 (1)	0.89
CS 7	6.96 (3)	1.27
CS 8	3.89 (3)	0.53
CS 9	10.10 (1)	1.42
CS 10	2.68 (1)	0.36
CS 11	2.80 (2)	0.78
CS 12	2.29 (1)	0.44
CS 13	3.89 (3)	0.53

NCS, non-corroded strand; CS, corroded strand; TPC, type of pit configuration.

Table 2 – Comparison of elongation between results from marker and machine.

Specimen	Elongation from marker (ε)	Adjusted elongation from machine (ε)
1	0.01	0.0089
2	0.0187	0.0217
3	0.0241	0.0236
4	0.035	0.0339
5	0.0093	0.0145
6	0.0183	0.0229
7	0.01	0.0089
8	0.011	0.01
9	0.0058	0.0038
10	0.0113	0.0161
11	0.0074	0.0039

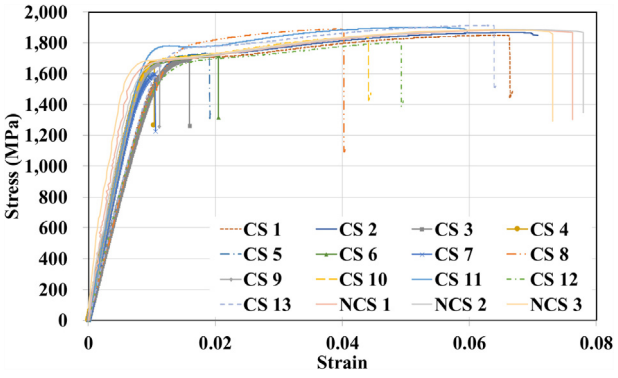

Fig. 5 – Stress–strain curves of corroded strands.

zone only focusing on the elongation. The elongation was measured after tensile test finished by vernier callipers from the distance between markers (see Fig. 4(c)). This elongation included the elastic shortening, therefore, the results from the machine were adjusted and compared by subtracting the elastic shortening. Table 2 shows the results of elongation. The average and standard deviation of differences between two results is 0.00254ε and 0.00175ε, respectively. Considering that the average of elongation is 3% of non-corroded strand which is 0.0752ε, the data from machine is considered acceptable.

Fig. 5 shows the stress–strain curves of corroded strands from tensile test, and it results that the ultimate strength and strain of the corroded strands decreases according to the extent of corrosion. However, the trend of the decrease seems to have different aspect from conventional studies on corrosion. As shown in Table 1, the section losses of the strands are not too much different (the greatest difference is 3.7%), while the difference of strain between non-corroded and corroded strands is about 0.065ε which is 87% of the strain capacity of

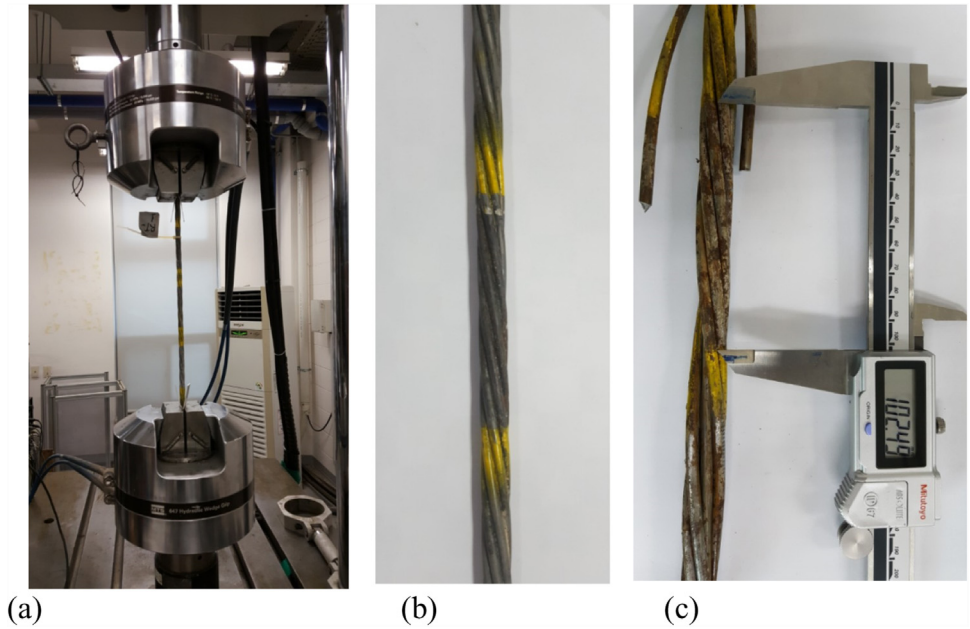

Fig. 4 – (a) Test setup, (b) Marker with 100 mm, and (c) Measuring with veriner callipers.

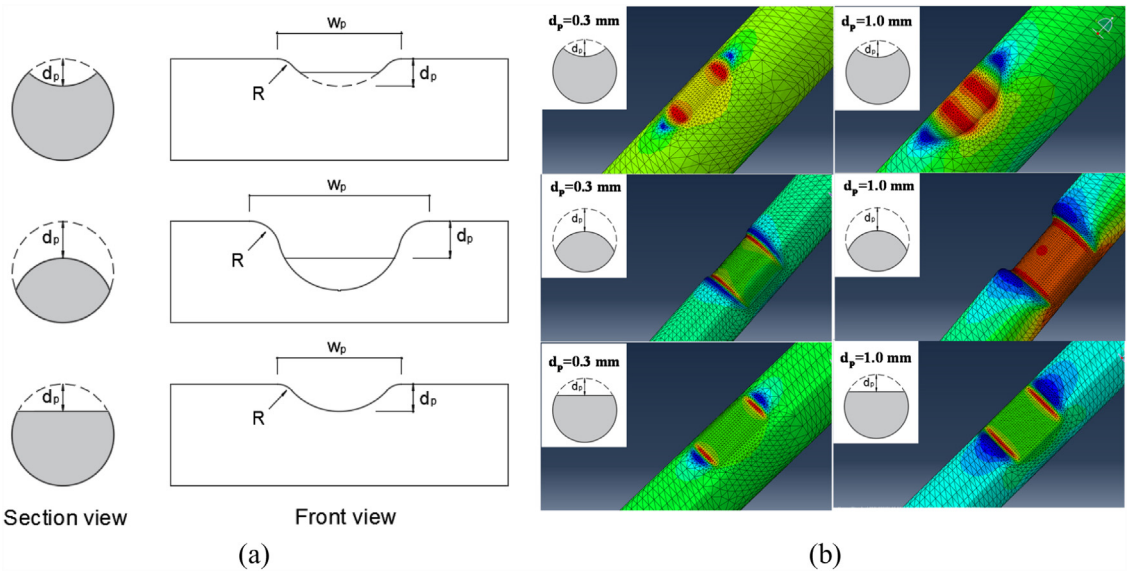

Fig. 6 – (a) Model design and (b) FEM model for corroded wire according to the pit configurations.

non-corroded strand. On the other hand, the section losses of wires are relatively greater difference (19.23% at most), and it leads to the assumption that most corroded wire governs the behaviour of the strand. To explain this assumption on the behaviour of corroded wire, it was decided to conduct finite element method (FEM) as below.

4. Finite element analysis

4.1. *Analysis model of corroded wire according to the pit configurations*

A strand consists of six outer wires and a core wire. This led to the assumption that the behaviour of a strand is combination of the behaviours of each wire. In this paper, FEM analysis was conducted to evaluate the mechanical behaviour of the wires if they have section loss according to the pit configurations in Fig. 3. Fig. 6 shows model design for corroded wire according to the pit configurations.

In Fig. 6, d_p is the depth of the pit, w_p is the width of the pit along the length, and R is the radius of fillet at the corner. The FEM models were made with various pit depth from 0.1 mm to 1.5 mm as shown in Fig. 6. The R and w_p were varied with type of pit depth and configuration to avoid local strain concentration. The length of the wire was modelled as 100 mm.

The material model of non-corroded strand was characterised by bi-linear curve to approximate the behaviour of non-corroded strands. The average mechanical properties of the three non-corroded stands from the tensile test are shown in Table 3. The Poisson's ratio is $\nu = 0.3$. Fig. 7 shows bi-linear material model derived from test results of non-corroded strand.

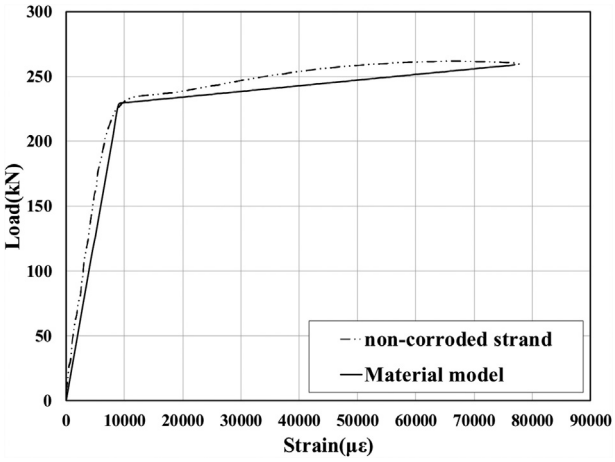

Fig. 7 – Bi-linear material model and test result of non-corroded strands.

4.2. *Analytical behaviour of corroded wires*

The finite element analysis models had been simulated using ABAQUS/Explicit under axial tensile loading until it stopped due to convergence problem. Arc length method as a numerical solution was used to guarantee that it simulated degradation behaviour after peak, because the purpose of this analysis was to estimate ultimate strength and strain.

Table 3 – Mechanical properties of non-corroded strand.

Elastic modulus E_s (MPa)	Yield strength f_y (MPa)	Yield strain ε_y	Ultimate strength f_u (MPa)	Ultimate strain ε_u
195,000	1628	0.0083	1865	0.075

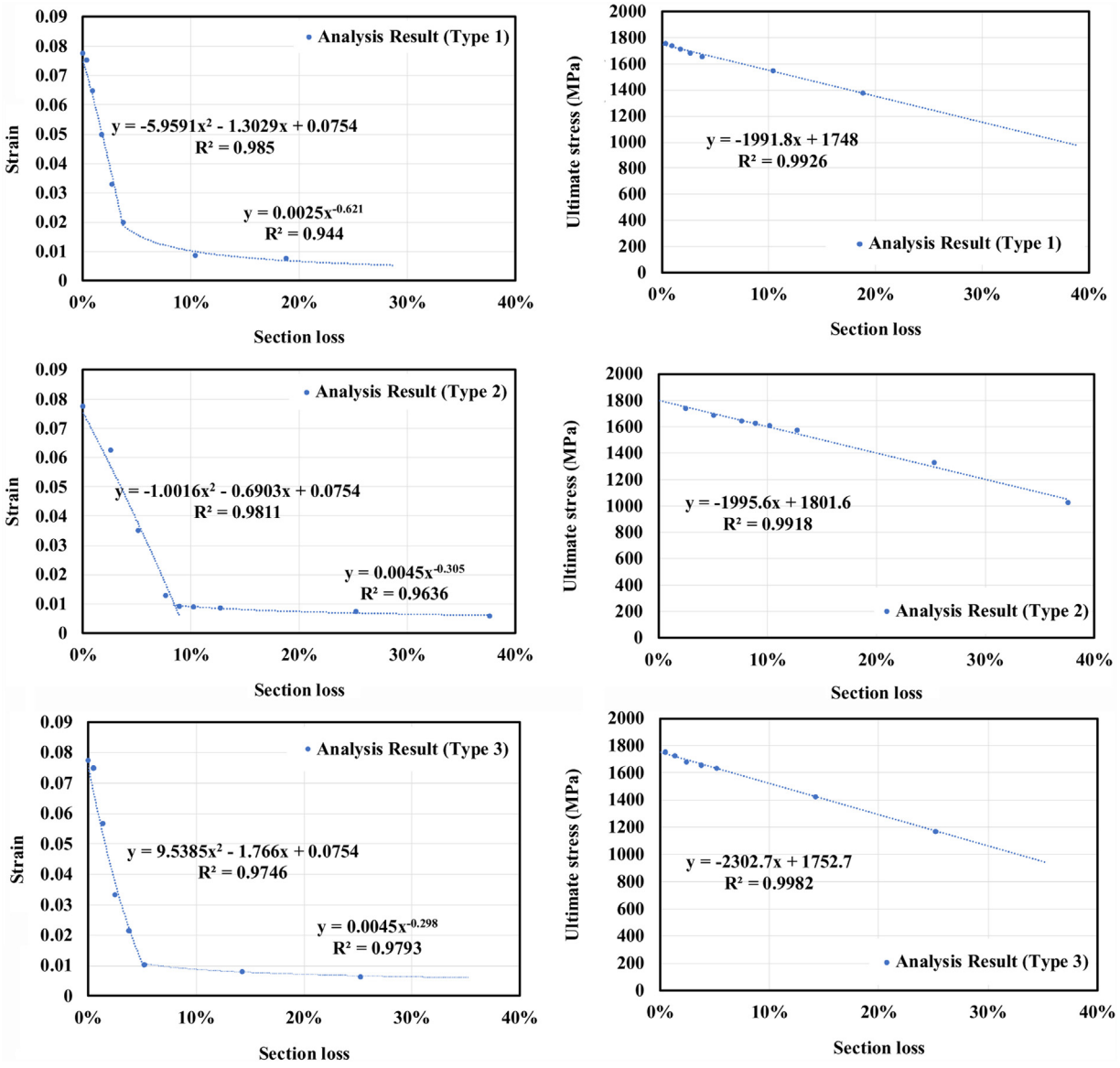

Fig. 8 – Reduction of ultimate stress and strain according to pit configurations.

The strand has seven wires, therefore, the result strength of wire analysis was considered as the sum of strength of wires when compared to the test result. The differences between test and analysis on non-corroded strand were 8.1% and 3.6% with respect to strength and strain, respectively. This can be acceptable considering the conservative evaluation.

For the mechanical properties of corroded strands with respect to the ultimate state, ultimate stress and strain reduction according to the section losses, calculated from Eqs. (1)–(6), was collected from analysis result of load-displacement relation (see Fig. 8). When stress was calculated, non-corroded section, which means no section loss, was considered so that the derived mechanical properties from the analysis result can be used to structural analysis of a member like girder without change of section property. This means only the change of material properties must be considered in a section of member including corroded strand without change of sectional area when structural analysis is conducted to analyse the

Table 4 – Coefficients for Eqs. (8) and (9).

Pit configuration	Coefficients						
	a	*b*	*c*	*d*	*e*	*f*	*g*
Type 1	−1991.8	1748.0	−5.96	−1.30	0.0754	0.0025	−0.621
Type 2	−1995.6	1801.6	−1.00	−0.69	0.0754	0.0045	−0.305
Type 3	−2302.7	1752.7	9.54	−1.77	0.0754	0.0045	−0.298

behaviour of the member because the mechanical properties already have information of change of sectional area of corroded strand. The relations between ultimate state properties and section loss were derived from regression analysis, and the stress reduction behaviour was expressed into two regions, because the behaviour is suddenly changed after the analysis models with pit depth of 0.5 mm.

5. Equivalent material model of corroded strands

5.1. *Stress–strain relation of corroded wires derived from analysis*

The stress-strain relation of a corroded wire was defined with bi-linear model. Eqs. (8) and (9) are the equations derived from regression analysis in Fig. 8 to define the ultimate state properties.

$$f_{u,c} = \alpha\eta + b \tag{8}$$

$$\varepsilon_{u,c} = \begin{cases} c\eta^2 + d\eta + e & for\ d_p < 0.5 \\ f\eta^g & for\ d_p \geq 0.5 \end{cases} \tag{9}$$

where $f_{u,c}$ and $\varepsilon_{u,c}$ are the ultimate stress and strain of corroded strand, respectively. η is section loss according to Eq. (7). The coefficients a, b, c, d, e, f, and g are defined from regression analysis with respect to pit configurations, which are shown in Table 4.

The yield stress and strain, in this paper, are defined as follows:

$$f_{y,c} = 0.85 f_{u,c} \tag{10}$$

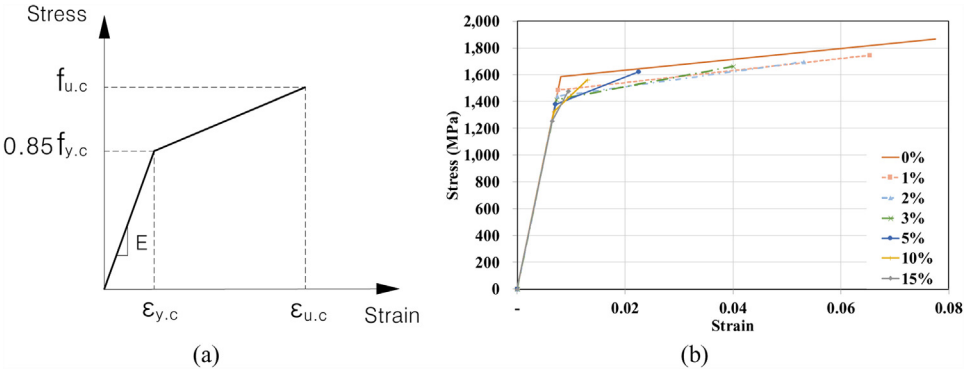

Fig. 9 – (a) Stress–strain relation of a corroded wire and (b) examples according to section loss regarding to type 1 pit configuration.

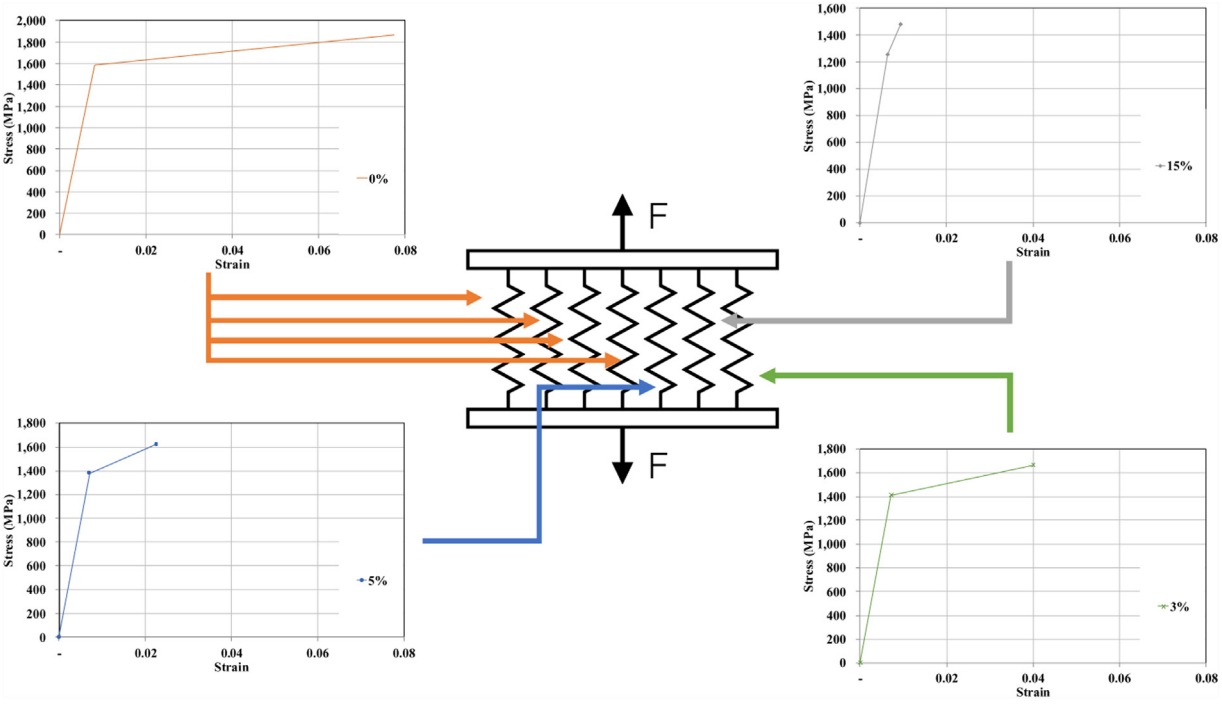

Fig. 10 – Spring model of a corroded strand composed by s-s relation of wires.

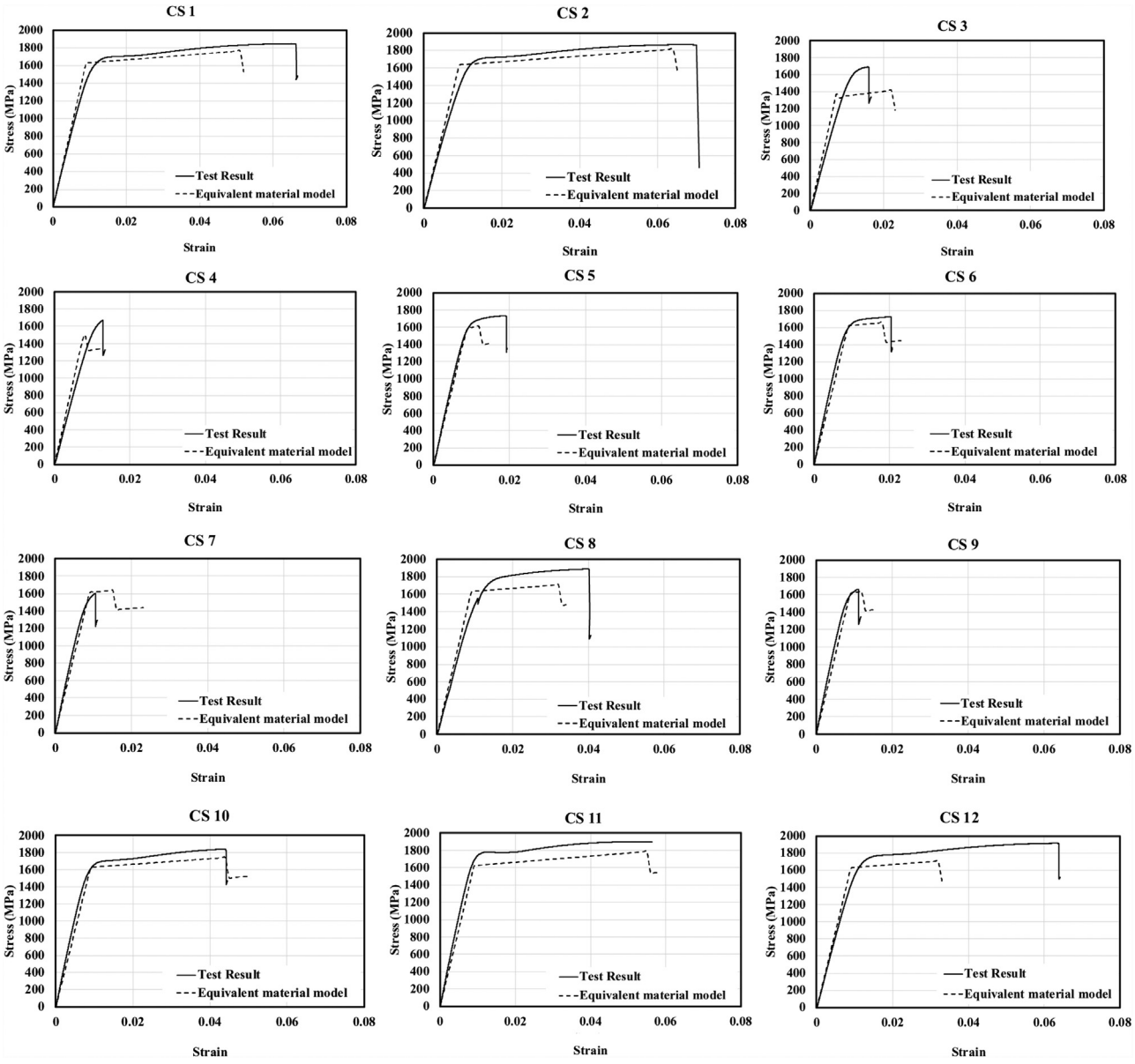

Fig. 11 – Comparison of the equivalent material model and test result.

$$\varepsilon_{y,c} = \frac{0.85 f_{u,c}}{E_s} \tag{11}$$

where $f_{y,c}$ and $\varepsilon_{y,c}$ are the yield stress and strain of corroded wire, respectively. $f_{u,c}$ and $\varepsilon_{u,c}$ are the ultimate stress and strain of corroded wire, respectively, from Eqs. (8) and (9). E_s is elastic modulus of a strand.

Using Eqs. (8), (9), (10), and (11), stress–strain relation of a corroded wire can be mathematically expressed as follows:

$$\sigma_w(\varepsilon) = \begin{cases} E_s \cdot \varepsilon & \varepsilon < \varepsilon_{y,c} \\ 0.85 f_{u,c} + \dfrac{\varepsilon - \varepsilon_{y,c}}{\varepsilon_{u,c} - s_{y,c}} 0.15 f_{u,c} & \varepsilon_{y,c} < \varepsilon \le \varepsilon_{u,c} \end{cases} \tag{12}$$

where $\sigma_w(\varepsilon)$ is the stress of a wire with respect to ε.

Fig. 9(a) shows the derived stress–strain curve for a corroded wire according to Eq. (12), and the examples of the stress-strain relations regarding to the pit configuration of type 1 are depicted in Fig. 9(b).

5.2. *Spring model of corroded strands for equivalent material model*

The strand, again, consists of six outer wires and a core wire, therefore, this paper suggested that the behaviour of a strand is a combination of the behaviour of each wire. Lu et al. [9] proposed a spring model for theoretical analysis of the behaviour of corroded strands, and this model is adopted in this paper (see Fig. 10) with assumptions as follow. First, the damage model of corroded strand is expressed with spring

model consists of a row of identical springs and rigid plate at both ends. Second, the friction behaviour between the surfaces of wires is neglected. Third, the external load or displacement should be shared uniformly and balanced to the springs. Fourth, each spring model has the behaviour of a wire defined by the stress–strain relation of Fig. 9(a). Fifth, the ultimate strength and strain of this model are determined when the weakest spring is reached its capacity. Sixth, the considered cross sectional area of each spring is only the area of intact wire without section loss because the section loss property is already considered in the derived stress–strain relation as explained in Chapter 4.2.

Base on the spring model, the equivalent material model for the corroded strand can be expressed as follows:

$$\sigma_s(\varepsilon) = \frac{\sum_{i=1}^{n} (\sigma_{w,i}(\varepsilon) A_{o,i})}{\sum_{i=1}^{n} (A_{o,i})} \quad (13)$$

where $\sigma_s(\varepsilon)$ is the stress of a strand with respect to ε. $\sigma_{w,i}(\varepsilon)$ is the stress of a ith wire making up the strand, and $A_{0,i}$ is the cross sectional area of the ith wire.

To verify the equivalent material model of corroded strand, Eq. (13), the results of tensile test in Fig. 5 were compared as shown in Fig. 11. Reduction of tensile strength of the corroded strand is well predicted by the proposed method. Considering irregularity and variance of corroded shape of wires, it can be said that the proposed equivalent material model of a strand with corroded wires is in reasonable agreement with the experimental results. The most important aspect of the mechanical behaviour of the corroded strand is the reduction of fracture strain of corroded wires. Therefore, the equivalent spring concept can be used for the assessment of prestressed concrete structures with corroded strands in terms of strength and deformation capacity.

6. Conclusion

In this paper, mechanical behaviour of corroded strands was estimated by detailed inspection, tensile tests and simplified analytical approach. The following conclusions are derived from the investigation.

1) The corrosion shape of a strand can be divided into three types of pit configurations, and equations to evaluate the sectional loss area are proposed in terms of the pit configurations.
2) Tensile strength and fracture strain of corroded strands were evaluated from tensile tests. The amount of decrease in tensile strength was larger than the amount of decrease in the reduction in cross sectional area, and the decrease of fracture strain was large enough to be cautious.
3) The stress-strain relations of corroded wire were derived from finite element analysis, which covers properties of pit configurations and various section losses.
4) A spring model including stress-strain relations of wires was adopted to simplify the evaluation and derive the equivalent material model of a corroded strand. It was verified that the equivalent material model estimated properly the strength and ductility of the corroded strand.

It is expected that the proposed method will be able to analytically evaluate the change in the structural behaviour of the concrete structure with corroded strand.

Conflicts of interest

The authors declare no conflicts of interest.

Acknowledgements

This study was supported by a grant (18SCIP-B128570-02) from the Smart Civil Infrastructure Research Program funded by the Ministry of Land, Infrastructure and Transport (MOLIT) of the Korean government and the Korea Agency for Infrastructure Technology Advancement (KAIA).

REFERENCES

[1] Bentur A, Diamond S, Berke N. Steel Corrosion in Concrete: Fundametals and Civil Engineering Practice. 1st ed; 1997. London.
[2] Chen Z, Zhang G, Bobaru F. The influence of passive film damage on pitting corrosion. J Electrochem Soc 2016;163:C19.
[3] Shamsad Ahmad. Reinforcement corrosion in concrete structures, its monitoring and service life prediction—a review. Cement Concr Compos 2003;25:459–71.
[4] Trejo D, Hueste MBD, Gardoni P, Pillai RG, Reinschmidt K, Im SB, Kataria S, Hurlebaus S, Gamble M, Ngo TT. Effect of voids in grouted post-tesioned concrete bridge construction: electrochemical testing and reliability assessment. Austin: Texas Transportation Institute; 2009.
[5] Reis RA. Corrosion evaluation and tensile results of selected post-tensioning strands at the SFOBB Skyway Seismic Replacement Project. Sacramento: California Department of Transportation; 2007.
[6] VDOT. Evaluation of grout and strands at 13 tendon locations and selected vertical Pt bars at fixed piers: maintenance and repair using corrosion mitigation systems (Final Report). Virginia Department of Transportation; 2013.
[7] ASTM G1-03. Standard practice for preparing, cleaning, and evaluating corrosion test specimens. West Conshohocken, PA: ASTM International; 2017.
[8] Wu X, Li H. Effect of strain level on corrosion of prestressing steel strands. In: Proceedings of International Association for Bridge and Structural Engineering. 2016. p. 292–9.
[9] Lu ZH, Li F, Zhao YG. An investigation of degradation of mechanical behaviour of prestressing strands subjected to chloride attacking. In: Proceedings of International Conference on Durability of Concrete Structures. 2016.
[10] ASTM G49-94. Standard guide for examination and evaluation of pitting corrosion. West Conshohocken, PA: ASTM International; 2005.
[11] Xia J, Jin WL, Zhao YX, Li LY. Mechanical performance of corroded steel bars in concrete. Struct Build 2013;166(5):235–46.
[12] Rinaldi Z, Imperatore S, Valente C. Experimental evaluation of the flexural behavior of corroded P/C beams. Construct Build Mater 2010;24:2267–78.
[13] Val DV, Melchers RE. Reliability of deteriorating RC slab bridges. J Struct Eng ASCE 1997;123(12):1638–44.
[14] Stewart MG. Mechanical behaviour of pitting corrosion of flexural and shear reinforcement and its effect on structural reliability of corroding RC beams. Struc Saf 2009;31:19–30.

[15] Hartt WH, Lee SK. Projecting corrosion-induced bridge tendon failure resulting from deficient grout: Part I–Model development and example results. Corrosion 2016;72(8):991–8.
[16] FHWA. Effect of voids in grouted, post-tensioned concrete bridge construction: volume 1—electrochemical testing and reliability assessment. Federal Highway Administration; 2009.
[17] PTI. Specification for grouting of post-tensioned structures. Post-Tensioning Institute; 2017.
[18] Kim JK, Kim JS, Kwon SH. Mechanical properties of a new prestressing strand with ultimate strength of 2160 MPa. KSCE J Civil Eng 2014;18(2):607–15.